

Arc Routing with Time-Dependent Travel Times and Paths

Thibaut Vidal

Departamento de Informtica, Pontifcia Universidade Catlica do Rio de Janeiro, vidalt@inf.puc-rio.br

Rafael Martinelli

Departamento de Engenharia Industrial, Pontifcia Universidade Catlica do Rio de Janeiro, martinelli@puc-rio.br

Tuan Anh Pham

ORLab, VNU University of Engineering and Technology, Vietnam
Military Logistics Research Center, Military Logistics Academy, Vietnam, ptanh@anvita.com.vn

Minh Hoàng Hà

ORLab, Faculty of Computer Science, Phenikaa University, Vietnam, hoang.haminh@phenikaa-uni.edu.vn

Technical Report, PUC-Rio

Vehicle routing algorithms usually reformulate the road network into a complete graph in which each arc represents the shortest path between two locations. Studies on time-dependent routing followed this model and therefore defined the speed functions on the complete graph. We argue that this model is often inadequate, in particular for arc routing problems involving services on edges of a road network. To fill this gap, we formally define the time-dependent capacitated arc routing problem (TDCARP), with travel and service speed functions given directly at the network level. Under these assumptions, the quickest path between locations can change over time, leading to a complex problem that challenges the capabilities of current solution methods. We introduce effective algorithms for preprocessing quickest paths in a closed form, efficient data structures for travel time queries during routing optimization, as well as heuristic and exact solution approaches for the TDCARP. Our heuristic uses the hybrid genetic search principle with tailored solution-decoding algorithms and lower bounds for filtering moves. Our branch-and-price algorithm exploits dedicated pricing routines, heuristic dominance rules and completion bounds to find optimal solutions for problem counting up to 75 services. Based on these algorithms, we measure the benefits of time-dependent routing optimization for different levels of travel-speed data accuracy.

Key words: Arc Routing Problem, Time-Dependent Travel Times, Combinatorial Optimization

1. Introduction

Congestion in city centers causes massive losses (400 billion dollars per year in the USA reported in Cookson and Pishue 2018) and a wide range of adverse effects on inhabitants. Transit times can widely vary during peak hours. With the widespread availability of sensors, mobile devices, and large databases of historical events, driving speeds can now be modeled more precisely to better optimize urban transportation in metropolitan areas. As a consequence, the amount of literature on vehicle routing problems considering time-dependent travel times (TDVRP) has quickly increased (Gendreau et al. 2015, Cattaruzza et al. 2017). However, we argue that current TDVRP models present major shortcomings.

1.1. Time-dependent Routing Models are Oversimplified

The wide majority of studies on TDVRP use a complete graph representation of the network in which each vertex corresponds to a service or depot location. In the seminal article of Ichoua et al. (2003), piecewise-constant vehicle speed functions are associated with the arcs of this complete graph to model time-dependent driving speeds. With these assumptions, a unique quickest path

is known to exist between any two locations. However, this is a rough approximation of reality. In practice, time-dependent speed profiles are specific to each street or region. In their survey and practitioners poll, Rincon-Garcia et al. (2018) highlighted that an inadequate management of time-dependent travel times represents the greatest current barrier to the adoption of vehicle routing software. As the capabilities of current solvers improve, it is increasingly important to account for vehicle speeds at the network level and use time-dependent quickest path calculations (Bast et al. 2016) to find travel-time *profiles* between service locations. In such conditions, the quickest path between two locations can change over time, but the FIFO property remains valid (Ghiani and Guerriero 2014), i.e., leaving earlier cannot result in a later arrival.

Very few TDVRP studies have considered time-dependent speed functions at the road network level. Eglese et al. (2006) and Maden et al. (2009) first introduced a road timetabling algorithm, called LANTIME, for TDVRPs with travel time information on streets. The performance of the algorithm was evaluated on road network data from South West England, leading to an estimated 7% savings in fuel. Huang et al. (2017) later proposed mathematical formulations for a TDVRP minimizing greenhouse gas emissions, in which the speed profiles are specific to each edge of the network. Finally, Jaballah et al. (2019) introduced a mathematical formulation and a simulated annealing solution approach for a TDVRP with time-dependent travel times at the network level.

The aforementioned studies focus on vehicle routing (i.e., node routing) scenarios. Yet, various applications for waste collection, road maintenance, and postal deliveries are more faithfully modeled with services on arcs and edges (Corberán and Laporte 2015). The resulting capacitated arc routing problems (CARP) require to take additional *mode* decisions, which represent the traversal direction of each service edge (Irnich 2008, Vidal 2017). These mode decisions influence the choice of entry and exit points for each service, and therefore the quickest paths. As discussed in Gendreau et al. (2015), time-dependent travel times have been largely ignored in the CARP literature, a surprising fact given that most related applications occur in urban contexts. Some research exists on mathematical formulations and solution methods for single-vehicle cases (Black et al. 2013, Sun et al. 2015, Yu and Lin 2015), but these methods remain limited to fairly small data sets counting around 25 services. In a nutshell, critical methodological challenges still need to be overcome to solve multi-vehicle time-dependent arc routing models at scale.

1.2. Towards a Time-dependent Capacitated Arc Routing Model

We introduce a formal definition of the time-dependent CARP (TDCARP) and propose state-of-the-art metaheuristics and mathematical programming algorithms to solve it. We consider a deterministic setting, assuming that travel speed estimates are available (i.e., based on traffic history) but will also consider, in our computational experiments, scenarios in which this information is inaccurate. Our travel speed functions are defined according to the IGP model of Ichoua et al. (2003), but they are specific to the edges of the road network. To our knowledge, this is the first extensive study on the CARP with time-dependent travel times at the network level.

Our metaheuristic is based on the unified hybrid genetic search (UHGS) with implicit service mode selection (Vidal et al. 2014, Vidal 2017). It relies on an incomplete solution representation, where service modes (edge traversal directions during services in our case) are optimized on the fly during every route evaluation by dynamic programming (DP). Our DP was adapted to account for time-dependent travel times. Moreover, we develop problem-tailored move evaluation lower bounds to filter non-promising moves during the local search. Our exact method is based on branch-cut-and-price (BCP). It exploits valid inequalities, stabilization, ng-route relaxation, tailored pricing algorithms —fast heuristic pricing, exact pricing with heuristic dominance, and exact pricing using completion bounds generated by backward pricing with maximum speed— as well as strong branching techniques. This method produces, for the first time, optimal solutions for TDCARP instances with up to 75 services. Our solution methods rely on the preprocessing of

continuous time-dependent quickest paths for all starting times, using a variant of Bellman-Ford algorithm in which continuous PL functions are maintained in closed form and updated through lower-envelope and composition operations. The resulting quickest path functions are maintained in bucket-based data structures to allow $\mathcal{O}(1)$ travel-times queries during routing solution. As a result, our algorithms do not need to use time discretization or perform numerous path calculations with fixed start times.

We conduct an extensive computational campaign on benchmark instances derived from the classical CARP benchmarks of Li and Eglese (1996), Beullens et al. (2003) and Brandão and Eglese (2008). We measure the benefits of time-dependent optimization in scenarios in which only approximate speed information is available. Therefore, our study gives a clear estimate of the benefits of time-dependent optimization and the impact of speed data quality. Summarizing, the main contributions of our work are the following.

- 1) We introduce a model of time-dependent service- and travel-time functions in the context of arc routing.
- 2) We design an effective algorithm to obtain the travel-time functions between origin-destination pairs in a closed form, without approximation or discretization, as well as efficient data structures to query these functions in near- $\mathcal{O}(1)$ elementary operations.
- 3) We propose efficient heuristic and exact solution approaches built upon innovative solution components (e.g., solution decoding algorithms, move filters, heuristic dominance, completion bounds), which have been specifically designed to be effective for the TDCARP.
- 4) We conduct extensive computational experiments to evaluate the performance of the proposed solution strategies and to measure the impact of time-dependent optimization with accurate or inaccurate speed information.

2. The Time-Dependent Capacitated Arc Routing Problem

Let $G = (V, E, A)$ be an undirected graph, in which V is a set of vertices, E is an edge set, and A is an arc set. Node $0 \in V$ represents a depot, where m vehicles of capacity Q are based and available at time 0. $E_R \subseteq E$ and $A_R \subseteq E$ represent edges and arcs requiring service, and $n = |E_R| + |A_R|$ represents the total number of services. Each service $u \in E_R \cup A_R$ is characterized by a nonnegative demand q_u . Each edge $u \in E_R$ can be serviced in one of its two possible orientations, called *modes* in Vidal (2017). In contrast, the orientation of services to arcs is fixed. To formalize this difference, we associate to each service u a mode set M_u representing its possible orientations, in such a way that $M_u = \{1, 2\}$ if $u \in E_R$ and $M_u = \{1\}$ otherwise. Each service should be performed exactly once, but any edge or arc of $E \cup A$ can be deadheaded multiple times while traveling in the network. Finally, the arcs and edges are characterized by time-dependent travel and service speed functions. As a consequence, the FIFO property is respected when traveling and servicing (i.e., starting later does not allow to arrive earlier), and waiting is never profitable (such that we can eliminate this possibility). The TDCARP aims to design up to m routes in such a way that:

- Each route starts and ends at vertex 0 (the depot);
- Each service is operated once by a single vehicle;
- The demand on each route does not exceed the vehicle capacity Q ;
- The duration of each route does not exceed a maximum value of D ;
- The sum of the route durations is minimized.

Speed model. In this work, we define time-dependent speed functions directly at the network level rather than on the complete graph representation. Therefore, given a planning horizon $[0, H]$, we associate to each arc and oriented edge $(i, j) \in A_R \cup E_R$ a distance d_{ij} along with a piecewise-constant speed function $v_{ij} : [0, D] \rightarrow \mathbb{R}^+$ with h_{ij} pieces representing the travel speed on this link as a function of time, i.e., the distance traveled per time unit. Speeds can change over time according

to these functions *while the vehicle is traveling* on a link. In these conditions, the FIFO property is known to hold (Orda and Rom 1990, Ichoua et al. 2003). We also introduce time-dependent travel and service time functions. For any $(i, j) \in A_R \cup E_R$, we define a positive piecewise-constant travel-and-service speed function $\hat{v}_{ij} : [0, D] \rightarrow \mathbb{R}^+$ with \hat{h}_{ij} pieces representing the distance *travelled and serviced* per time unit. Asymmetric edge speeds are allowed, such that possibly $v_{ij}(t) \neq v_{ji}(t)$ and $\hat{v}_{ij}(t) \neq \hat{v}_{ji}(t)$. Different arcs and edge orientations can therefore have different speed functions and different breakpoints.

Based on these definitions, the arrival time values $\Phi_{ij}(t_i)$ and $\hat{\Phi}_{ij}(t_i)$ at j when departing from i at t_i are calculated as:

$$\Phi_{ij}(t_i) = \left\{ x \left| \int_{t_i}^x v_{ij}(t) dt = d_{ij} \right. \right\} \quad \text{when travelling on } (i, j) \quad (1)$$

$$\hat{\Phi}_{ij}(t_i) = \left\{ x \left| \int_{t_i}^x \hat{v}_{ij}(t) dt = d_{ij} \right. \right\} \quad \text{when servicing } (i, j). \quad (2)$$

In a similar manner, the departure time values $\Phi_{ij}^{-1}(t_j)$ and $\hat{\Phi}_{ij}^{-1}(t_j)$ from i to arrive at j exactly at time t_j are calculated as:

$$\Phi_{ij}^{-1}(t_j) = \left\{ x \left| \int_x^{t_j} v_{ij}(t) dt = d_{ij} \right. \right\} \quad \text{when travelling on } (i, j) \quad (3)$$

$$\hat{\Phi}_{ij}^{-1}(t_j) = \left\{ x \left| \int_x^{t_j} \hat{v}_{ij}(t) dt = d_{ij} \right. \right\} \quad \text{when servicing } (i, j). \quad (4)$$

3. Methodology

We separate the description of our solution methods in four sub-sections: 1) the calculation of a closed-form representation for arrival time functions, 2) the preprocessing of quickest path profiles, 3) our exact branch-cut-and-price approach for the TDCARP, and 4) our hybrid genetic search metaheuristic, designed to produce high-quality heuristic solutions in a controlled amount of time.

3.1. Continuous Travel Time Functions

All solution algorithms for vehicle routing with time-dependent travel times need efficient methods for travel time queries. When travel time information is provided at the network level, computationally-demanding travel time calculation methods can become a major obstacle to the application of routing optimization algorithms (Vidal et al. 2020). Two types of queries are recurrent in the solution process. For this reason, they should be performed as quickly as possible:

- *Travel and service time queries*: evaluating $\Phi_{ij}(t)$ or $\hat{\Phi}_{ij}(t)$ on an arc (i, j) at a given time t ;
- *Quickest path queries*: evaluating the earliest arrival time $\Psi_{ij}(t)$ at a node j from a node i at a starting time t .

Most TDVRP algorithms use an iterative algorithm for travel time queries requiring $\mathcal{O}(h_{ij})$ time (see Appendix A). To avoid this overhead, we preprocess continuous representations of Φ_{ij} and $\hat{\Phi}_{ij}$ as closed-form piecewise-linear (PL) functions and develop efficient data structures which allow queries in $\mathcal{O}(1)$ time in most situations. We first state two important properties of the arrival time functions, and then proceed with a description of our approach.

Property 1 Functions Φ_{ij} are piecewise linear, continuous and monotonic.

Proof. This follows directly from Equation (1) given that functions v_{ij} are piecewise-constant, positive and bounded. \square

Property 2 Let $t_1, \dots, t_{h_{ij}-1}$ be the breakpoints of function v_{ij} . Function Φ_{ij} has up to $2(h_{ij}-1)$ breakpoints with values $t_1, \dots, t_k, \Phi_{ij}^{-1}(t_l), \dots, \Phi_{ij}^{-1}(t_{h_{ij}-1})$ where $k = \arg \max\{x \mid t_x \leq \Phi_{ij}^{-1}(D)\}$ and $l = \arg \min\{x \mid t_x \geq \Phi_{ij}(0)\}$.

Proof. Define $V_{ij}(x) = \int_0^x v_{ij}(t) dt$. V_{ij} and its inverse V_{ij}^{-1} are non-negative strictly-increasing PL functions. V_{ij} has breakpoints t_1, \dots, t_k where $k = \arg \max\{x \mid t_x \leq \Phi_{ij}^{-1}(D)\}$ and V_{ij}^{-1} has breakpoints $V(t_l), \dots, V(t_{h_{ij}-1})$ where $l = \arg \min\{x \mid t_x \geq \Phi_{ij}(0)\}$. Based on Equation (1), we obtain $V_{ij}(\Phi_{ij}(t)) - V_{ij}(t) = d_{ij}$ leading to:

$$\Phi_{ij}(t) = V_{ij}^{-1}(V_{ij}(t) + d_{ij}). \quad (5)$$

Function Φ_{ij} is PL as a composition of two PL functions. Breakpoints can occur whenever t is a breakpoint of $V_{ij}(t)$, or whenever $V_{ij}(t) + d_{ij}$ is a breakpoint of V_{ij}^{-1} . In the latter case, there exists k such that $V_{ij}(t) + d_{ij} = V_{ij}(t_k)$, i.e., such that $t = \Phi_{ij}^{-1}(t_k)$. \square

Theorem 2 holds for function Φ_{ij} as well as $\hat{\Phi}_{ij}$. Its characterization of the breakpoints leads to a simple procedure to generate a closed-form representation of Φ_{ij} (or $\hat{\Phi}_{ij}$) in $\mathcal{O}(h_{ij}^2)$ time. This procedure, described in Algorithm 1, is performed once for each link $(i, j) \in A \cup E$ in a preprocessing phase, before the quickest path algorithm and routing solution method.

Algorithm 1: Closed-form construction of Φ_{ij}

```

k ← arg max{x | t_x ≤ Φij-1(D)}
l ← arg min{x | t_x ≥ Φij(0)}

ABP = ∅
ABP ← (0, Φij(0))
for x ∈ {1, ⋯, k} do ABP ← (t_x, Φij(t_x))           ▷ O(hij) queries to Algo 3
for x ∈ {l, ⋯, hij - 1} do ABP ← (Φij-1(t_x), t_x)   ▷ O(hij) queries to Algo 4
ABP ← (Φij-1(D), D)

APIECES = ∅
SORT AND REMOVE DUPLICATES(ABP)                       ▷ O(hij log hij)
for x ∈ {1, ⋯, SIZE(ABP) - 1} do APIECES ← (ABP[x], ABP[x + 1])
return APIECES

```

The result can be stored as a simple array of function pieces, giving indexed access in $\mathcal{O}(1)$ time if the index of the piece is known, and $\mathcal{O}(\log h_{ij})$ otherwise by binary search. To further reduce the query complexity, we divide the planning horizon into B buckets and create an auxiliary array whose i^{th} element points towards the function piece that contains time $(i-1)\frac{D}{B}$. Any travel time query from a time t is resolved by comparing the buckets of indices $\lfloor t/B \rfloor$ and $\lceil t/B \rceil$: if both buckets point towards the same piece, then this piece is returned in $\mathcal{O}(1)$ time, otherwise a binary search is initiated between the pieces and completed in $\mathcal{O}(\log h_{ij})$ time.

3.2. Travel Time Profile Queries

Quickest path queries constitute an essential building block of vehicle routing and arc routing algorithms applied to real networks. In most applications, a complete $n \times n$ travel-time matrix is preprocessed to guarantee $\mathcal{O}(1)$ time, cost, or distance queries through the search. Time-dependent travel times defined at the network level greatly increase the complexity of such preprocessing.

Indeed, travel times between origin-destination pairs now depend on an additional continuous parameter, the start time, and the quickest paths may change over time (Ghiani and Guerriero 2014). As a consequence, previous studies did not exploit preprocessing and instead relied on time-consuming quickest-path queries during routing solution. This computational overhead drastically limited the number of local-search moves and construction decisions that can be evaluated in a fixed amount of time, such that only simplistic algorithms, based on much fewer local-search iterations, were practical (Jaballah et al. 2019).

To circumvent this issue, we use a *continuous* preprocessing approach, during which we compute closed-form representations of the arrival time $\Psi_{ij}(t)$ function at each destination j for all departure times t at origin i . This effectively avoids the computational overhead of approaches based on iterative travel time queries as well as the memory overhead and imprecision of approaches based on time discretization. Since the FIFO assumption holds in our context, we use a dynamic programming approach that follows the same scheme as the classical Bellman-Ford algorithm, but in which the discrete labels are replaced by continuous PL functions. This procedure, described in Algorithm 2, is applied from the depot and every vertex located at the end of a serviced arc or at one extremity of a serviced edge.

Algorithm 2: Quickest path algorithm from i for all starting times

```

for  $j \in V$ ,  $\Psi'_{ij} = \Psi_{ij} = \begin{cases} \text{id} & \text{if } i = j \\ \infty & \text{otherwise} \end{cases}$ 
 $\mathcal{L} \leftarrow \{i\}$ 
while  $\mathcal{L} \neq \emptyset$  do
  for  $(x, y) \in E \cup A : x \in \mathcal{L}$  do
     $\Psi'_{iy} \leftarrow \text{LOWERENVELOPE}(\Psi'_{iy}, \Phi_{xy} \circ \Psi_{ix})$ 
   $\mathcal{L} \leftarrow \emptyset$ 
  for  $y \in V$  do
    if  $\Psi_{iy} \neq \Psi'_{iy}$  then
       $\mathcal{L} \leftarrow \mathcal{L} \cup y$ 
       $\Psi_{iy} \leftarrow \Psi'_{iy}$ 

```

In Algorithm 2, “id” represents the identity function. Due to the continuous representation of functions $\Psi_{ij}(t)$, each usual label comparison is replaced by a lower envelope operation (Hershberger 1989), and the “o” operation corresponds to the composition of two PL functions. These operations are directly performed on the closed-form representation of the functions. The total number of lower envelope and composition operations remains limited to $O(|V|(|E \cup A|))$ as in Bellman-Ford algorithm, yet the number of function pieces may grow in the worst case as $n^{\Theta(\log n)}$ (Foschini et al. 2014). As discussed in Section 4.2, the number of pieces obtained in our computational experiments remains sufficiently small to be efficiently computed and stored in a few seconds.

As a result of this algorithm, we obtain the continuous PL functions Ψ_{ij} representing the *value* of the quickest paths from any vertex i at any time t , and store them using the bucket data structure described in Section 3.1. We do not maintain the time-dependent *paths* themselves, since 1) this information is only useful at the end of routing optimization to produce the detailed solution, 2) this would lead to a significant memory overhead and 3) one can simply use a discrete time-dependent quickest path algorithm for fixed departure times between each pair of successive vertices in the final solution to recover the paths.

3.3. Branch-Cut-and-Price Algorithm

Our branch-and-price algorithm exploits the same set partitioning model as for most vehicle routing problems. The critical differences with other works occur in the definition of the pricing problem, the labeling algorithms designed to solve it, the branching rules, and the selection of valid inequalities.

Let Ω be the set of all feasible routes for the TDCARP. Each feasible route $r \in \Omega$ is defined as a sequence of required links (oriented services) $((i_1, j_1), (i_2, j_2), \dots, (i_k, j_k))$ starting and ending at the depot. Equation (6) permits to calculate the time of each service as well as the route completion time (return to the depot) as $\Phi_r = \Psi_{j_k 0}(T(i_k, j_k))$:

$$\begin{cases} T(i_\ell, j_\ell) = \hat{\Phi}_{i_\ell j_\ell}(\Psi_{j_{\ell-1} i_\ell}(T(i_{\ell-1}, j_{\ell-1}))) \\ T(i_1, j_1) = \hat{\Phi}_{i_1 j_1}(\Psi_{0 i_1}(0)). \end{cases} \quad (6)$$

Let λ_r be a binary variable taking value 1 if and only if route $r \in \Omega$ is used in the solution. Moreover, let a_{ij}^r be a binary parameter which takes value 1 if and only if route r performs service (i, j) . The set partitioning formulation of the TDCARP can be written as follows:

$$\min \sum_{r \in \Omega} \Phi_r \lambda_r \quad (7)$$

$$\text{s.t.} \quad \sum_{r \in \Omega} \lambda_r = m \quad (8)$$

$$\sum_{r \in \Omega} a_{ij}^r \lambda_r = 1 \quad \forall (i, j) \in E_R \cup A_R \quad (9)$$

$$\lambda_r \in \{0, 1\} \quad \forall r \in \Omega. \quad (10)$$

Equation (7) minimizes the total duration of the routes. Constraint (8) sets a limit on the number of available vehicles, and Constraints (9) ensure that each service is performed exactly once.

Valid Inequalities. Firstly, we use a lifting of the classical odd-edge cutset cuts for the CARP (Belenguer and Benavent 1998). In its original form, this family of cuts works on any subset S of nodes with an odd number of incident required links ($|\delta_R(S)|$ odd), by imposing the number of incident deadheaded links ($\delta(S)$) to be at least one. Bartolini et al. (2013) proved that this family of cuts can be lifted by imposing the same condition on the paths between two required links. Let $\tilde{G} = (\tilde{V}, \tilde{A})$ be a complete graph, called the *deadheaded graph*, where $\tilde{A} = \{(i, j) | i \in V \wedge j \in V, i \neq j\}$, and \tilde{b}_{ij}^r is a binary parameter taking value 1 if and only if route r deadheads the path from i to j after servicing a required link finishing at i and about to start a service on a required link at j . Then, the lifted odd-edge cutset cuts can be defined as in Equation (11):

$$\sum_{(i,j) \in \delta(S)} \tilde{b}_{ij}^r \lambda_r \geq 1 \quad \forall S \subseteq V \setminus \{0\}, |\delta_R(S)| \text{ odd}. \quad (11)$$

Secondly, we use a lifting of the classical capacity cuts (Belenguer and Benavent 1998). This lifting can be obtained by considering another complete graph $\tilde{G} = (\tilde{V}, \tilde{A})$, called the *required graph*, where $\tilde{V} = E_R \cup A_R \cup \{0\}$ and $\tilde{A} = \{(u, v) | u \in \tilde{V} \wedge v \in \tilde{V}, u \neq v\}$, i.e., a complete graph where the nodes are the required links plus a node representing the depot. We further use the lower bound on the number of vehicles required to service a set $S \subseteq \tilde{V} \setminus \{0\}$, represented by $k(S)$, and a binary parameter \tilde{b}_{uv}^r which is 1 if route r services required link v after required link u . A capacity cut defined over this graph, as shown in Equation (12), is similar to a capacitated vehicle routing problem (CVRP) capacity cut. These cuts, proposed by Bartolini et al. (2013), are a lifting of the original CARP capacity cuts.

$$\sum_{(u,v) \in \delta(\tilde{S})} \tilde{b}_{uv}^r \lambda_r \geq 2k(S) \quad \forall S \subset \tilde{V} \setminus \{0\} \quad (12)$$

Column Generation. Formulation (7–10) has an exponential number of variables and requires column generation (CG). At each iteration of the CG, the linear relaxation of the set partitioning formulation is solved, and possible negative reduced-cost variables are detected by a pricing algorithm and included in the formulation. The process is iterated until no negative reduced costs variable exists. The reduced costs are computed from the dual information associated with the current solution, using the dual variables γ , β_{ij} , ρ_{ij} and π_{uv} associated with Constraints (8), (9), (11) and (12).

Our pricing algorithm is based on dynamic programming. It computes all candidate paths that start at the depot and that can lead to a negative reduced-cost route. For simplicity, the depot will be represented as a fictitious link (i_0, j_0) . Any path $P = ((i_0, j_0), (i_1, j_1), (i_2, j_2), \dots, (i_h, j_h))$ is represented by a label $\mathcal{L}(P) = (i(P), j(P), q(P), \Phi(P), \xi(P), \Pi(P))$, containing the last link $(i(P), j(P))$, the total load $q(P)$, the arrival time at the last vertex $\Phi(P)$, the cumulated value of the dual variables, calculated as $\xi(P) = \gamma + \sum_{\ell=1}^h (\beta_{i_\ell j_\ell} + \rho_{j_{\ell-1} i_\ell} + \pi_{(i_{\ell-1}, j_{\ell-1})(i_\ell, j_\ell)})$, and the set $\Pi(P)$ of serviced links. An extension from a path P to a link (i_ℓ, j_ℓ) is feasible if and only if $q(P) + q_{(i_\ell, j_\ell)} \leq Q$, $\hat{\Phi}_{i_\ell j_\ell}(\Psi_{j(P) i_\ell}(\Phi(P))) \leq D$ and $(i_\ell, j_\ell) \notin \Pi(P)$. This extension produces a new label given in Equation (13). At the end of the pricing algorithm, we obtain the routes from the paths such that $(i(P), j(P)) = (i_0, j_0)$ and compute their reduced costs as $\bar{c}(P) = \Phi(P) - \xi(P)$.

$$\mathcal{L}(P') = \left(i_\ell, j_\ell, q(P) + q_{(i_\ell, j_\ell)}, \hat{\Phi}_{i_\ell j_\ell}(\Psi_{j(P) i_\ell}(\Phi(P))), \right. \\ \left. \xi(P) + \beta_{i_\ell j_\ell} + \rho_{j(P) i_\ell} + \pi_{(i(P), j(P))(i_\ell, j_\ell)}, \Pi \cup (i_\ell, j_\ell) \right) \quad (13)$$

The number of paths considered in the pricing algorithm can grow very quickly. To mitigate this effect, we use the following rule to discard dominated paths.

Exact dominance: Path P_1 exactly dominates path P_2 if:

- | | | | |
|-------|------------------------------|------|-------------------------------|
| (i) | $j(P_1) = j(P_2)$ | (iv) | $\xi(P_1) \geq \xi(P_2)$ |
| (ii) | $q(P_1) \leq q(P_2)$ | (v) | $\Pi(P_1) \subseteq \Pi(P_2)$ |
| (iii) | $\Phi(P_1) \leq \Phi(P_2)$. | | |

This exact dominance rule uses separate comparisons for the arrival time at the last vertex $\Phi(P)$ and the cumulated value of the dual variables $\xi(P)$. These two comparisons appear to be necessary to avoid eliminating promising labels. Consider the following example with two paths: P_1 with $\Phi(P_1) = 10$ and $\xi(P_1) = 1$, and P_2 with $\Phi(P_2) = 20$ and $\xi(P_2) = 10$. Suppose that $j(P_1) = j(P_2)$, $q(P_1) \leq q(P_2)$ and $\Pi(P_1) \subseteq \Pi(P_2)$. In this example, the reduced costs are $\bar{c}(P_1) = 10 - 1 = 9$ and $\bar{c}(P_2) = 20 - 10 = 10$. If we test $\bar{c}(P_1) \leq \bar{c}(P_2)$ instead of Rules (iii) and (iv), path P_1 would appear to dominate P_2 . However, if an extension exists to a link (i_ℓ, j_ℓ) for which $\beta_{i_\ell j_\ell} + \rho_{j(P_1) i_\ell} + \pi_{(i(P_1), j(P_1))(i_\ell, j_\ell)} = 1$, $\hat{\Phi}_{i_\ell j_\ell}(\Psi_{j(P_1) i_\ell}(\Phi(P_1))) = 3$, and $\hat{\Phi}_{i_\ell j_\ell}(\Psi_{j(P_2) i_\ell}(\Phi(P_2))) = 1$ (possible due to the time-dependent travel times), then the reduced costs of paths P_1 and P_2 after the extension become $10 + 3 - (1 + 1) = 11$ and $20 + 1 - (10 + 1) = 10$, respectively. In this case, a promising label would have been discarded.

Due to this additional comparison, the TDCARP dominance rule eliminates much fewer labels than the typical CARP dominance based on simple reduced cost comparison. To improve this behavior, we propose the following heuristic dominance rule:

Heuristic dominance: Path P_1 heuristically dominates path P_2 if:

- | | | | |
|-------|------------------------------|------|---|
| (i) | $j(P_1) = j(P_2)$ | (iv) | $\xi(P_1) + \mu(\Phi(P_2) - \Phi(P_1)) \geq \xi(P_2)$ |
| (ii) | $q(P_1) \leq q(P_2)$ | (v) | $\Pi(P_1) \subseteq \Pi(P_2)$ |
| (iii) | $\Phi(P_1) \leq \Phi(P_2)$. | | |

Discussion. In rule (iv) of the heuristic dominance, parameter μ is a positive scalar which weights the contribution of an earlier arrival time at the current link to the final reduced cost at the end of the route. Indeed, it makes sense to assume that an earlier arrival time can lead to a smaller reduced cost at the end of the route. However, as highlighted in Appendix B, arrival time differences can expand or contract over a path by an arbitrary amount, making it difficult to estimate the value of a time gain (or a bound thereof) for an incomplete route. Because of this, the pricing algorithm based on this dominance is only a heuristic. We use it in a first CG phase with a factor $\mu = 0.5$ until no negative cost column is found, and then we switch to the exact pricing algorithm with the exact dominance. During our computational experiments, we observed that only one iteration of the exact pricing was needed in 89% of the cases, i.e., only to *prove* that the CG is completed.

Relaxing elementarity. To further reduce the computational time of the pricing algorithm, we use a variant of the *ng*-route relaxation instead of imposing elementarity (Baldacci et al. 2011). For each required link, the approach builds a list of the “closest” required links considering an estimated distance measure between two links. Given the required links (i_1, j_1) and (i_2, j_2) , the estimated distance between them is $\hat{\Phi}_{i_1 j_1}(0)/2 + \Psi_{j_1 i_2}(0) + \hat{\Phi}_{i_2 j_2}(0)/2$. The procedure then considers the minimum between the four possible combinations of service directions. For each required link, we keep the four “closest” required links, including itself (i.e., the size of the *ng*-sets is set to four).

Backward pricing and completion bounds. It is not possible to use bidirectional pricing in the TDCARP without keeping (and dominating) speed functions on each label (Lera-Romero et al. 2020). However, we can still obtain completion bounds information from a backward pricing algorithm considering the maximum speed for each link. From its dynamic programming matrix, we build a matrix $\mathcal{B}(i, j, q, t)$ containing the best reduced cost from the backward paths that end before service (i, j) , with load up to $Q - (q - q_{(i,j)})$, using time up to $\lceil D - (t - \hat{\Phi}_{ij}^+) \rceil$, where $\hat{\Phi}_{ij}^+$ is the servicing time of (i, j) on maximum speed. We then use this information to fathom forward label $\mathcal{L}(P)$ if $\bar{c}(P) + \mathcal{B}(i(P), j(P), q(P), \lceil t(P) \rceil) \geq 0$.

Stabilization. The convergence of the column generation is also improved by applying a dual stabilization procedure. In this work, we use a simple approach that uses a stabilization factor $\alpha \in [0, 1[$, as in Pessoa et al. (2010). The factor is used on each column generation iteration to perform a convex combination on the dual information from the last iteration and the current one. Our procedure starts with a value of 0.9, which gives a higher weight to the last iteration dual information. When the optimal solution of the pricing algorithm is not a route with a negative reduced cost, the stabilization factor value is decreased in 0.1, and the pricing algorithm is called again. This procedure is considered until the factor reaches zero.

Fast heuristic pricing. At the beginning of every column generation iteration, we rely on a fast heuristic pricing to quickly generate promising columns. This procedure is also based on dynamic programming, but it only maintains the path with the best reduced cost for every link and load value (Martinelli et al. 2014). Only when this routine fails to find routes with negative reduced cost, the column generation calls the exact pricing, starting with the heuristic dominance, and terminating with the exact dominance.

Branch-and-bound. The column generation method solves the linear relaxation of Formulation (7–10). Even with the valid inequalities (11) and (12), integer solutions are not guaranteed and a branch-and-bound approach is required. Thus, whenever a feasible solution is found, we test if this solution is a valid integer solution by checking the arcs on the required graph. If any arc variable has a fractional value, we branch. As discussed in Pecin and Uchoa (2019), testing the integrality on the required graph is sufficient to guarantee the correctness of the solution.

In addition, we use three branching rules, (i) on the deadheaded degree of a vertex $v \in V$, (ii) on the value of an arc $(i, j) \in \hat{A}$, and (iii) on the value of an arc $(v, w) \in \hat{A}$. The first branching

rule follows the same reasoning as the odd-edge cutset cuts (11). If a vertex $v \in V$ has an even (or odd) number of incident required links, then the number of incident deadheaded links must also be even (or odd, respectively). The other two branching rules are straightforward. The choice of branching rules is made using strong branching. A subset of candidates with up to 50 elements is built, and for each candidate, the column generation is solved using only the fast heuristic pricing. Let z_c^L and z_c^R be the objective value of the left and right siblings of candidate c , respectively. The procedure selects, as in Røpke (2012), the candidate with highest ranking based on the formula of Equation (14) with $\alpha = 3/4$.

$$\text{RANK}(c) = \alpha \min(z_c^L, z_c^R) + (1 - \alpha) \max(z_c^L, z_c^R) \quad (14)$$

A new branch with two nodes is then created, and the entire column generation is solved, including the valid inequalities. The next node to explore is obtained following the best-bound strategy.

3.4. Hybrid Genetic Search

As observed in our experiments, our branch-cut-and-price algorithm optimally solves most problem instances with up to 75 services in a few minutes. Still, it fails to solve larger instances due to limited memory and time. Optimal solutions of this scale are invaluable for experimental comparisons and validations, but remain insufficient for most applications.

To produce solutions for larger instances as well as initial upper bounds, we introduce an efficient population-based metaheuristic. Our algorithm follows the same principles as the Unified Hybrid Genetic Search (UHGS), which effectively combines crossover-based solution generation, local search, and population-diversity management to produce high-quality solutions for numerous vehicle-routing and arc-routing problem variants (Vidal et al. 2014). The recent application of the UHGS principle to the family of arc-routing problems (Vidal 2017) exploits two other key strategies: 1) an indirect solution representation in the local search, in which each route is represented as a sequence of services, with an exact decoding algorithm to find optimal mode choices, and 2) efficient lower-bounds to filter non-promising moves in amortized $\mathcal{O}(1)$ time. Our adaptation of this method to the TDCARP requires replacing the solution decoder and lower bounds while retaining the same solution representation and search operators. For the sake of brevity, we concentrate our description on the new solution decoder (Section 3.4.1) and lower bounds (Section 3.4.2) and refer to Vidal (2017) for a description of the general search strategy which remains identical. Moreover, an open-source implementation of the complete TDCARP algorithm is provided at <https://github.com/vidalt/HGS-TDCARP>.

3.4.1. Indirect Solution Representation and Search Space. Indirect solution representations and decoders have been instrumental in designing state-of-the-art solution approaches for optimization problems mixing different decision-variables classes (Vidal et al. 2015a, 2016, Vidal 2017, Herszterg et al. 2019, Mecler et al. 2019, Toffolo et al. 2019). As illustrated in Figure 1, the goal of an indirect solution representation is the same as a projection-based problem decomposition. By representing the solution with a smaller subset of decision variables and systematically using an optimal (e.g., dynamic programming-based) decoder to complete the solution, the heuristic searches a smaller space while the rest of the decisions are taken exactly. This representation simplifies the solution approach by making it more structured and greatly reduces the approximations inherent to heuristic search.

The TDCARP combines four classes of decisions: ASSIGNMENT of services to vehicles, SEQUENCING of the services within each route, MODE choices for the services (i.e., choices of directions for the services on edges), and PATH choices between the services. Each of these decision sets contains a number of options that grows exponentially with the number of services. Moreover, in contrast with the TDVRP where services correspond to nodes in the network, the quickest paths between the

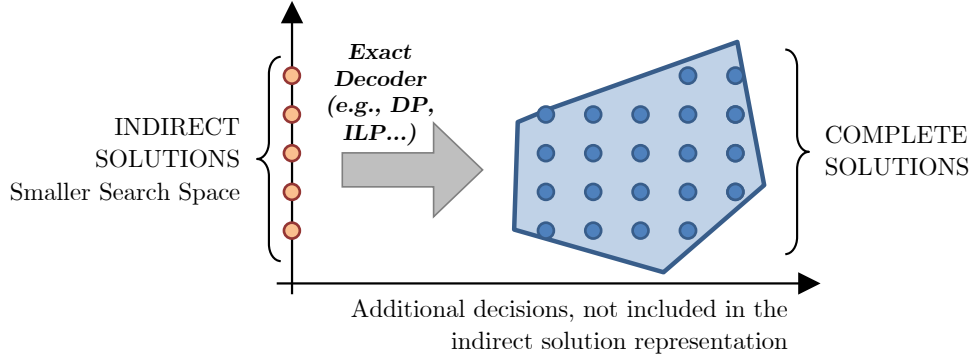


Figure 1 Indirect solution representation and decoding

extremities of successive edge services in the TDCARP are conditioned by the choices of service orientations, i.e., the MODE decisions.

To efficiently optimize the MODE decisions, we use the same solution representation as Vidal (2017), in which a solution is represented as sequences of services (routes) without their mode information, and systematically use a dynamic programming decoding algorithm to complete the solutions. Figure 2 compares this representation choice (R-INDIRECT) with a classical complete solution representation (R-COMPLETE).

	<u>R-COMPLETE</u>	<u>R-INDIRECT</u>
	ASSIGNMENT, SEQUENCES and MODES	only ASSIGNMENT and SEQUENCES
Number of solutions in search space	$N_{\text{CVRP}} \times 2^{ E_R }$ N_{CVRP} representing the number of solutions of a CVRP instance with n customers	N_{CVRP}
Decoder	Iterative propagation of time-dependent travel times (example with $k = 3$ services): 	Time-dependent quickest path for a discrete departure date in an acyclic auxiliary graph (example with $k = 3$ services to edges):

Figure 2 Solution representations, search spaces and decoders

Due to the time-dependent travel times, solution evaluations require to propagate arrival and service completion times over the auxiliary graph illustrated in Figure 2 (rightmost side). In R-INDIRECT, this propagation is done using Bellman's algorithm in topological order, using the information of the quickest paths Ψ from the preprocessing step to evaluate the travel times between edge extremities (black edges on Figure 2), as well as the service time functions $\hat{\Phi}$ (gray edges). For a route $\sigma = (\sigma(1), \dots, \sigma(|\sigma|))$ represented according to R-INDIRECT as a sequence of services starting and ending at the depot (such that $\sigma(1) = 0$ and $\sigma(|\sigma|) = 0$), the completion time $T_{\sigma(i)}^{\text{EXACT}}[x]$ of each service $\sigma(i)$ for each mode $l \in M_{\sigma(i)}$ can be calculated as:

$$T_{\sigma(i)}^{\text{EXACT}}[l] = \begin{cases} 0 & \text{if } i = 1 \\ \min_{k \in M_{\sigma(i-1)}} \{ \hat{\Phi}_{\sigma(i)}^l(\Psi_{\sigma(i-1)\sigma(i)}^{kl}(T_{\sigma(i-1)}^{\text{EXACT}}[k])) \} & \text{otherwise,} \end{cases} \quad (15)$$

and the route duration is given by $T_{\sigma(|\sigma|)}^{\text{EXACT}}[1]$.

In Equation (15), $\Psi_{ij}^{kl}(t)$ represents the arrival time when leaving the end of service i in mode k at time t towards the origin of service j in mode l , and $\hat{\Phi}_i^l(t)$ represents the completion time of service i in mode l starting at time t . Let C_Ψ and $C_{\hat{\Phi}}$ be the complexity of querying the arrival time functions Ψ and the service time functions $\hat{\Phi}$, respectively. With this notation, route evaluations in R-INDIRECT take $4kC_\Psi + 4kC_{\hat{\Phi}}$ time, in comparison to $(k+1)C_\Psi + kC_{\hat{\Phi}}$ time for R-COMPLETE. This is a fourfold increase of evaluation effort, but it dramatically reduces the size of the search space (by a factor $2^{|E_R|}$) and renders MODE and PATH decisions optimal and transparent within the search. As will be discussed in the next section, the computational effort of route evaluations can be further mitigated with move filters based on route-cost lower bounds, and their evaluation by preprocessing and concatenation.

3.4.2. Efficient Local Search. Local searches maintain an incumbent solution s and explore a neighborhood $\mathcal{N}(s)$ obtained by testing some changes on s , called moves. The local search of UHGS uses a first improvement policy in which $\mathcal{N}(s)$ is explored in random order, and any improving move is directly applied. It uses classical intra-route and inter-route moves: 2-OPT, 2-OPT*, as well as RELOCATE and SWAP of 0, 1 or 2 consecutive services with possible reversals, subject to proximity restrictions (Laporte et al. 2014, Vidal et al. 2013, 2014). We now recall two properties which are fundamental to efficiently filter moves in the TDCARP, and then proceed with the definition of the bounds.

Property 3 All the considered moves consist of disconnecting up to two routes of the incumbent solution s into a constant number of sequences of consecutive visits and concatenating these sequences in a different order (Vidal et al. 2015b). Preprocessing auxiliary information on the sequences of consecutive visits from s can help to reduce the evaluation complexity of routes obtained from their concatenations.

Property 4 Let Π be a move which transforms a pair of routes (σ_1, σ_2) into (σ'_1, σ'_2) . Let $C_{\text{LB}}(\sigma)$ be a lower bound on the cost of a route σ . If $C_{\text{LB}}(\sigma'_1) + C_{\text{LB}}(\sigma'_2) - C(\sigma_1) - C(\sigma_2) \geq 0$, then Π is non-improving and can be filtered out.

Lower bounds on move evaluations for the TDCARP. To efficiently evaluate move lower bounds, our method uses preprocessing and concatenation principles and therefore maintains auxiliary information on the sequences of consecutive services from s . More precisely, any sequence of consecutive visits σ is characterized by a lower bound $T^{\text{LB}}(\sigma)[k, l]$ on the travel and service time over σ , starting the first service in mode k and finishing the last service in mode l , for each mode combination. This information is calculated by induction. It is preprocessed at the start of the local search and updated after each change in the solution s using a simple lexicographic calculation method over the services. For a sequence σ containing a single service i , we have:

$$T^{\text{LB}}(\sigma)[k, l] = \begin{cases} \min_{t \in [0, D]} \{\hat{\Phi}_i^k(t) - t\} & \text{if } k = l \\ \infty & \text{otherwise.} \end{cases} \quad (16)$$

In this equation, $\min_{t \in [0, D]} \{\hat{\Phi}_i^k(t) - t\}$ is a scalar which represents the minimum time needed to operate service i in mode k . This value can be easily collected from the closed-form service-time function and subsequently accessed in $\mathcal{O}(1)$. Now, these bounds can be evaluated for larger sequences of services $\sigma_1 \oplus \sigma_2$ arising from the concatenation of any two sequences σ_1 and σ_2 :

$$T^{\text{LB}}(\sigma_1 \oplus \sigma_2)[k, l] = \min_{x, y} \left\{ T^{\text{LB}}(\sigma_1)[k, x] + \min_{t \in [0, D]} \{\Psi_{\sigma_1(|\sigma_1|)\sigma_2(1)}^{xy}(t) - t\} + T^{\text{LB}}(\sigma_2)[y, l] \right\}. \quad (17)$$

Equation (17) provides a lower bound on the shortest time needed to perform σ_1 followed by σ_2 , starting and finishing in modes k and l respectively. This equation is used to preprocess the data (by iteratively appending one node) and to evaluate the moves as a concatenation of existing sequences. It is important to remark that $\min_{t \in [0, D]} \{\Psi_{ij}^{xy}(t) - t\}$ used in this equation represents the value of the quickest path *at the best starting time* t between the end extremity of service i in mode x and the starting extremity of service j in mode y . This value is obtained as a by-product of the calculation of the continuous quickest-path functions Ψ (prior to the routing optimization phase, as discussed in Section 3.2). It gives a much tighter travel-time bound than a discrete shortest path algorithm on the network that fixes arc and edge lengths to their minimum travel time values over the planning horizon.

Finally, we can strengthen our bound by remarking that, in a route $\sigma_1 \oplus \dots \oplus \sigma_S$ obtained by the concatenation of S sequences, the exact arrival time values (without any approximation) over the first sequence are known from the current incumbent solution s . The resulting lower bound is:

$$T^{\text{LB}^+}(\sigma_1 \oplus \dots \oplus \sigma_S) = \min_{x,y} \left\{ \Psi_{\sigma_1(l|\sigma_1)\sigma_2(1)}^{xy} (T_{\sigma_1(l|\sigma_1)}^{\text{EXACT}}[x]) + T^{\text{LB}}(\sigma_2 \oplus \dots \oplus \sigma_S)[y, 1] \right\} \quad (18)$$

For a route composed of S sequences, calculating this lower bound requires four evaluations of the travel time functions Ψ as well as a constant number of additions proportional to S . The lower bound evaluation is thus one order of magnitude faster than the exact move evaluation. Our algorithm first evaluates this lower bound for each route involved in a move and possibly rejects this move based on Property 4, otherwise it subsequently uses Equation (15) for an exact time evaluation. In our experiments, this strategy permits to filter 91% of the moves, to such an extent that exact move evaluations do not represent anymore a search bottleneck.

4. Computational Experiments

We conduct extensive computational experiments with two main objectives.

- 1) We evaluate the performance of the proposed algorithms as well as the effectiveness of some of their principal components: the continuous quickest-path procedure, the pricing using heuristic dominance and completion bounds in the BCP, as well as the efficient structures for travel time queries and lower bounds used to filter local-search moves in HGS.
- 2) We measure the impact of time-dependent routing and path optimization, considering different levels of speed inaccuracies.

4.1. Experimental Setup and Benchmark Instances

All methods from this paper were implemented in C++, using CPLEX 12.8 for the solution of the master problems and linear programs in our BCP algorithm. The tests were conducted on a single thread of an Intel Core i7-8700K 3.70GHz CPU.

For our analyses, we generated three classes of TDCARP benchmark instances with different levels of time dependency. The network information, customer demands, and vehicle capacities were extracted from the first ten BMCV data sets (C01–C10, from Beullens et al. 2003) built from Flanders road network, and from ten EGL data sets (Li and Eglese 1996, Brandão and Eglese 2008) associated with a winter gritting case study in Lancashire. For each of these 20 data sets, we generated three instances with different degrees of time dependency: low (L), medium (M), and high (H). In each case, the piecewise-constant speed profile $v_{ij}(t)$ of each link (i, j) was generated by randomly selecting six distinct breakpoints in $\{0.05D, 0.1D, 0.15D, \dots, 0.95D\}$, and then randomly selecting a speed value for each function segment $k \in \{1, \dots, 7\}$ from a uniform distribution $U(a_k, b_k)$ parametrized as indicated in Table 1. Finally, we assumed that travel-and-service speed represents 70% of deadheading speed, i.e., $\hat{v}_{ij}(t) = 0.7 \times v_{ij}(t)$ for all $(i, j) \in E \cup A$, and used the same fleet-size limit as the original CARP data sets.

k	Type L	Type M	Type H
1	[0.6,0.9]	[0.5,0.8]	[0.4,0.7]
2	[0.8,1.0]	[0.7,1.0]	[0.6,1.0]
3	[1.0,1.3]	[1.0,1.4]	[1.0,1.6]
4	[0.9,1.1]	[0.8,1.2]	[0.7,1.3]
5	[1.0,1.3]	[1.0,1.4]	[1.0,1.6]
6	[0.8,1.0]	[0.7,1.0]	[0.6,1.0]
7	[0.6,0.9]	[0.5,0.8]	[0.4,0.7]

Table 1 Parameters $[a_k, b_k]$ for the generation of the speed scenarios

4.2. Performance of the Time-dependent Quickest Path Algorithm

We evaluate the performance of the continuous quickest-path algorithm presented in Section 3.2. Since this algorithm is only run during preprocessing, its results may be retained for successive routing solutions (e.g., for different customer sets) as long as the speed estimates are unchanged. Figure 3 reports the total CPU time spent by the algorithm as well as the average number of function pieces in the resulting Φ functions (over all origin-destination pairs) for each of the three instance categories. To evaluate the asymptotical behavior of the algorithm, we fitted these values as a power-law $f : |V| \rightarrow \alpha|V|^\beta$ via a least-squares regression of an affine function on the log-log graph.

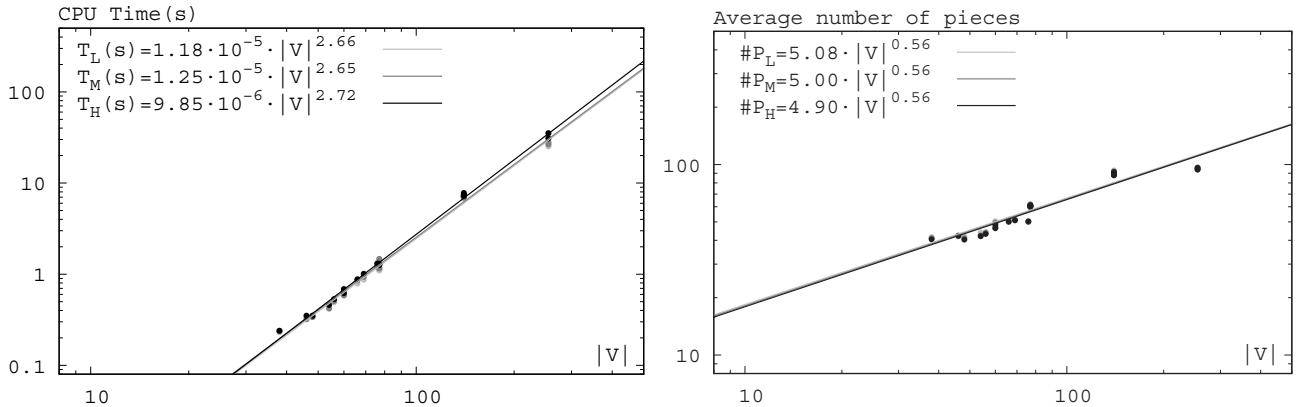


Figure 3 Performance of the continuous quickest path algorithm for instances with low (L), medium (M) and high (H) time dependency

Based on these results, we observe that the magnitude of the time dependency (L, M, and H) has only a limited impact on the performance of the quickest-path algorithm. The time needed to preprocess the continuous quickest-paths for all origin-destination pairs grows as $|V|^x$ with $2.65 \leq x \leq 2.72$ and remains smaller than 40 seconds on all test instances. Moreover, the average number of function pieces for all origin-destination pairs only grows in $|V|^{0.56}$, reaching approximately 100 pieces in the largest instances. These average-case observations contrast with worst-case analyzes predicting an exponential growth (Foschini et al. 2014). To further reduce the preprocessing time whenever needed, the quickest-path algorithm could also be applied in parallel (calculating quickest-paths from different origins on different processors), or replaced by more sophisticated approaches based on contraction hierarchies (Batz et al. 2013, Bast et al. 2016).

4.3. Performance of the Branch-Cut-and-Price Algorithm

Next, we evaluate the performance of the BCP algorithm. Tables 2 to 4 present its computational performance for the low, medium, and high time dependency instances, excluding the largest two data sets from Brandão and Eglese (2008) with 347 and 375 services, for which the root-node CG could not be completed. The results are divided into two groups: Root Node and Branch-Cut-and-Price. In each group, columns LB, Gap, and T(s) respectively represent the lower bound, the percentage gap, and the time in seconds. For the complete BCP algorithm, the additional columns UB, N_E , N_H , R, and C represent the upper bound, the number of BCP nodes explored with exact pricing, the number of BCP nodes explored with the fast heuristic pricing during strong branching, the number of routes and cuts. The percentage gaps are calculated as $100 \times (UB - LB) / LB$. It is also important to observe that the BCP algorithm starts with the UB found by the metaheuristic, and that no further improvement on this solution was obtained for any instance.

Inst	$ E_R $	Root Node			Branch-Cut-and-Price							
		LB	Gap	T(s)	LB	UB	Gap	T(s)	N_E	N_H	R	C
C01	79	2350.97	1.28%	55.26	2365.23	2381.01	0.67%	21599.70	163	4870	20074	748
C02	53	1869.36	0.26%	13.16	1874.24	1874.24	0.00%	131.24	15	432	4246	200
C03	51	1592.70	0.60%	41.03	1602.26	1602.26	0.00%	549.93	19	480	4956	211
C04	72	1953.48	0.31%	131.38	1959.58	1959.58	0.00%	4377.85	39	1191	12658	373
C05	65	2485.97	0.94%	26.57	2509.43	2509.43	0.00%	18320.00	183	5620	16306	596
C06	51	1570.26	0.15%	29.11	1572.59	1572.59	0.00%	371.37	13	393	6204	199
C07	52	2058.63	0.58%	16.80	2070.49	2070.49	0.00%	277.25	17	501	4165	345
C08	63	1880.55	1.02%	21.27	1899.67	1899.67	0.00%	2191.33	87	2596	8482	604
C09	97	3329.41	0.63%	304.26	3345.64	3350.24	0.14%	21599.70	118	3586	17581	759
C10	55	2126.94	1.71%	5.81	2163.26	2163.26	0.00%	660.77	79	2317	5378	478
Avg C		2121.83	0.75%	64.46	2136.24	2138.28	0.08%	7007.91	73	2199	10005	451
egl-e1	51	1618.94	0.56%	41.58	1627.97	1627.97	0.00%	877.12	33	852	5049	244
egl-e2	72	2327.27	0.67%	138.07	2339.52	2342.83	0.14%	21599.70	230	6711	11970	630
egl-e3	87	2875.33	1.01%	255.83	2895.57	2904.36	0.30%	21599.70	191	5575	12574	811
egl-e4	98	3305.87	1.07%	270.04	3323.42	3341.41	0.54%	21599.70	219	6383	11013	832
egl-s1	75	2289.11	0.25%	256.43	2294.85	2294.85	0.00%	2489.01	25	714	6352	414
egl-s2	147	4361.29	0.49%	886.99	4369.29	4382.64	0.31%	21598.50	101	2991	10778	1986
egl-s3	159	4608.44	0.55%	1750.46	4615.94	4633.79	0.39%	21598.50	59	1677	9489	903
egl-s4	190	5470.11	1.21%	1573.58	5477.57	5536.26	1.07%	21598.40	62	1757	9900	1187
Avg egl		3357.05	0.73%	646.62	3368.02	3383.01	0.34%	16620.08	115	3333	9641	876

Table 2 Performance of the BCP algorithm on low time-dependency instances.

These results show that the amount of time-dependency has some impact on the BCP algorithm. With low time-dependency, eight optimal solutions are obtained for the instances C01–C10 and two for the EGL instances, leading to ten optimal solutions overall out of the 20 instances. In comparison, nine and eight optimal solutions have been found for the medium and high time-dependency cases, respectively. A study of the relative gaps confirms our observations: for the low time-dependency case, an average relative gap of 0.74% is achieved at the root node, with a final average gap of 0.26%. In contrast, the root node gap increases to 0.85% and 1.02% for the medium and high time-dependency cases, and the final average gap rises to 0.28% and 0.37%. We also noted that the number of non-dominated labels explored during pricing at the root node is 30% larger, on average, on the instances of type H than on the instances of type L. Finally, only a single call to the exact pricing algorithm was needed for 98.37% of the nodes in type-L instances (i.e., only to prove that the CG is completed), whereas this ratio drops to 77.61% for type-H instances.

Inst	$ E_R $	Root Node			Branch-Cut-and-Price							
		LB	Gap	T(s)	LB	UB	Gap	T(s)	N_E	N_H	R	C
C01	79	2401.73	0.92%	92.07	2417.71	2423.80	0.25%	21599.70	169	5009	18296	807
C02	53	1882.00	0.75%	13.90	1896.14	1896.14	0.00%	1049.45	69	2129	7879	367
C03	51	1626.26	0.71%	67.76	1637.80	1637.80	0.00%	1082.72	27	762	5768	209
C04	72	1986.64	0.51%	110.18	1996.75	1996.75	0.00%	5089.53	53	1538	13986	427
C05	65	2504.32	0.57%	21.58	2518.55	2518.55	0.00%	199.43	17	478	3630	258
C06	51	1581.11	0.06%	35.10	1582.08	1582.08	0.00%	100.40	5	120	3483	149
C07	52	2095.72	1.09%	18.62	2118.61	2118.61	0.00%	822.74	55	1595	5980	427
C08	63	1922.56	1.18%	17.48	1945.23	1945.23	0.00%	1975.13	97	2822	7438	562
C09	97	3368.35	1.16%	507.60	3389.81	3407.54	0.52%	21599.70	130	3932	15574	742
C10	55	2163.62	2.03%	5.62	2207.63	2207.63	0.00%	1472.44	149	4482	6730	555
Avg C		2153.23	0.90%	88.99	2171.03	2173.41	0.08%	5499.12	77	2287	8876	450
egl-e1	51	1645.35	0.48%	45.46	1653.19	1653.19	0.00%	1446.37	41	1082	4811	252
egl-e2	72	2374.09	0.79%	184.52	2388.03	2392.91	0.20%	21599.70	213	6396	10608	701
egl-e3	87	2925.54	1.04%	222.93	2946.82	2956.03	0.31%	21599.60	215	6232	12588	584
egl-e4	98	3415.99	1.03%	367.68	3430.98	3451.16	0.59%	21599.70	203	5939	10310	566
egl-s1	75	2368.82	0.55%	328.14	2378.22	2381.80	0.15%	21598.60	177	5269	13931	653
egl-s2	147	4490.65	0.53%	975.90	4501.01	4514.46	0.30%	21598.50	129	3825	10822	1330
egl-s3	159	4746.62	0.58%	2405.09	4753.27	4774.16	0.44%	21598.40	37	1089	8630	935
egl-s4	190	5606.52	1.32%	3525.89	5612.43	5680.67	1.22%	21598.40	47	1373	9877	1470
Avg egl		3446.70	0.79%	1006.95	3457.99	3475.55	0.40%	19079.91	133	3901	10197	811

Table 3 Performance of the BCP algorithm on medium time-dependency instances.

Inst	$ E_R $	Root Node			Branch-Cut-and-Price							
		LB	Gap	T(s)	LB	UB	Gap	T(s)	N_E	N_H	R	C
C01	79	2416.45	1.15%	82.77	2431.77	2444.24	0.51%	21599.80	213	6211	18006	701
C02	53	1877.57	0.65%	24.79	1889.78	1889.78	0.00%	281.57	29	915	4584	223
C03	51	1637.28	0.62%	77.36	1647.38	1647.38	0.00%	1400.63	27	773	5474	151
C04	72	1988.62	1.20%	102.67	2010.97	2012.42	0.07%	21599.80	155	4470	21694	609
C05	65	2484.81	0.83%	16.81	2505.37	2505.37	0.00%	8776.53	253	7784	12179	509
C06	51	1563.85	0.15%	44.35	1566.24	1566.24	0.00%	225.20	9	216	3939	154
C07	52	2124.90	1.34%	14.53	2153.38	2153.38	0.00%	2118.14	123	3584	7313	395
C08	63	1938.63	1.09%	17.82	1959.71	1959.71	0.00%	4523.27	147	4303	9396	563
C09	97	3362.46	1.74%	645.53	3384.05	3420.94	1.09%	21599.70	132	3962	13146	564
C10	55	2178.21	2.29%	6.54	2228.00	2228.00	0.00%	12399.90	361	10873	10910	821
Avg C		2157.28	1.10%	103.32	2177.67	2182.74	0.17%	9452.45	145	4309	10664	469
egl-e1	51	1659.50	0.71%	53.88	1671.31	1671.31	0.00%	1519.80	51	1401	4353	247
egl-e2	72	2406.54	1.00%	176.47	2426.65	2430.55	0.16%	21599.60	236	7010	9232	504
egl-e3	87	2950.62	0.95%	285.06	2969.42	2978.79	0.32%	21599.70	229	6693	10822	587
egl-e4	98	3524.30	0.89%	601.84	3537.15	3555.56	0.52%	21599.60	133	3992	8941	575
egl-s1	75	2402.08	0.88%	515.27	2417.04	2423.32	0.26%	21598.60	195	5727	10668	644
egl-s2	147	4602.66	0.82%	1499.58	4613.70	4640.30	0.58%	21598.50	89	2665	9846	1073
egl-s3	159	4808.35	0.66%	1717.51	4816.24	4840.15	0.50%	21598.50	84	2509	8636	965
egl-s4	190	5694.69	1.35%	5239.66	5700.98	5771.63	1.24%	21598.50	37	1147	9706	1100
Avg egl		3506.09	0.91%	1261.16	3519.06	3538.95	0.45%	19089.10	132	3893	9026	712

Table 4 Performance of the BCP algorithm on high time-dependency instances.

Sensitivity analysis. Our BCP relies on new methodological components that were carefully tailored for the TDCARP. We evaluate the impact of two key strategies: the exact pricing using heuristic dominance (HD) and the backward pricing + completion bounds (CB). Therefore, we compare BCP with two alternative configurations named BCP-noHD and BCP-noCB in which these components were deactivated. Tables 5 and 6 analyze the computational time of the three

methods on the 27 instances which can be solved to optimality, as well as their final optimality gap on the remaining open instances.

T(s)	BCP	BCP-noHD	BCP-noCB
Median	1400.63	1637.62	3588.61
Average	2767.74	2965.61	5964.68
# Better	—	20	27
# Equal	—	0	0
# Worse	—	7	0

Table 5 Comparison: Computational time

Gap(%)	BCP	BCP-noHD	BCP-noCB
Median	0.39	0.40	0.55
Average	0.48	0.48	0.60
# Better	—	13	27
# Equal	—	5	0
# Worse	—	9	0

Table 6 Comparison: Final gap

As visible in this sensitivity analysis, the use of the exact pricing with heuristic dominance contributes to a reduction of computational effort on 20 instances out of 27. Its effectiveness remains still limited by the necessity of exact dominance to complete the pricing process. In contrast, the contribution of the backward pricing and completion bounds is visible for all instances, as it directly impacts the computational efficiency of the exact dominance phase. This approach considerably speeds up the solution process, permitting a more thorough search until the time limit and a substantial reduction of the final gap on open instances.

4.4. Performance of the Hybrid Genetic Search

To evaluate the performance of the HGS, we run it ten times with different seeds on all instances, and compare its solutions with the lower bounds and optimal solutions (LB/Opt) obtained by the BCP. Tables 7 to 9 report the results of this experiment. The leftmost columns report the instance names, number of services, and the known LB/Opt solution. Known optimal solutions are highlighted in boldface. The next columns report the CPU time spent calculating the quickest-path information. Finally, the remaining columns report the average and best solution quality of the HGS over the ten runs, the gap between the average and best solution values of the HGS, the gap between the average solution values of the HGS and the LB/Opt, and finally the CPU time of the HGS.

As visible in these experiments, the HGS produces solutions of consistently good quality within a limited computational effort. 26 out of 27 optimal solutions have been attained on every run, whereas the optimal solution of the remaining instance (M-C05) has been attained on six runs out of ten. For the remaining instances which have no known optimum, the HGS finds average solutions that are guaranteed to be no further than 1.46% from the optimum, based on the available lower bounds. The gap between average and best solutions over ten runs amounts to 0.08% on average over all instances. This shows that the solution quality of the algorithm is stable over multiple executions. The HGS takes an average time of five minutes for the BMCV instances (C01–C10) and 31 minutes for the EGL instances. Faster runs could be achieved, if needed, by reducing the termination criterion, the population size, or by parallelizing some operations (e.g., generating multiple solutions in parallel). Finally, the level of time dependency has only a minor impact on computational performance: comparing the results on the instances with low (L) and high (H) time dependency, we observe a moderate increase of CPU time (by 24%) but no significant deterioration of solution quality.

Next, we analyze the move lower bounds used to quickly filter non-improving moves (Equation 18) and the bucket structure used for fast travel times queries. Figure 4 represents, for each time-dependency level and instance, the percentage of moves that needed exact evaluation, and the percentage of travel time queries that needed a binary search.

Inst	$ E_R $	BCP LB/Opt	SP T(s)	HGS				T(s)
				Best	Avg	Gap	Gap _{LB}	
C01	79	2365.23	0.87	2381.01	2381.16	0.01%	0.67%	556.31
C02	53	1874.24	0.34	1874.24	1874.24	0.00%	0.00%	119.40
C03	51	1602.26	0.33	1602.26	1602.26	0.00%	0.00%	183.26
C04	72	1959.58	0.63	1959.58	1959.58	0.00%	0.00%	256.15
C05	65	2509.43	0.49	2509.43	2509.43	0.00%	0.00%	166.92
C06	51	1572.59	0.23	1572.59	1572.59	0.00%	0.00%	282.54
C07	52	2070.49	0.47	2070.49	2070.49	0.00%	0.00%	105.58
C08	63	1899.67	0.79	1899.67	1899.67	0.00%	0.00%	129.31
C09	97	3345.64	1.18	3350.24	3350.24	0.00%	0.14%	479.55
C10	55	2163.26	0.58	2163.26	2163.26	0.00%	0.00%	104.42
Avg C			0.59			0.00%	0.08%	238.34
egl-e1	51	1627.97	1.10	1627.97	1627.97	0.00%	0.00%	149.81
egl-e2	72	2339.52	1.15	2342.83	2342.83	0.00%	0.14%	346.51
egl-e3	87	2895.57	1.12	2904.36	2906.18	0.06%	0.37%	423.22
egl-e4	98	3323.42	1.11	3341.41	3341.67	0.01%	0.55%	694.42
egl-s1	75	2294.85	6.86	2294.85	2294.85	0.00%	0.00%	298.37
egl-s2	147	4369.29	7.06	4382.64	4383.58	0.02%	0.33%	1195.87
egl-s3	159	4615.94	6.70	4633.70	4641.87	0.18%	0.56%	3181.89
egl-s4	190	5477.57	7.05	5524.07	5547.14	0.42%	1.27%	3520.23
egl-g1	347	—	25.17	5659.43	5667.57	0.14%	—	3600.12
egl-g2	375	—	28.49	6543.11	6571.46	0.43%	—	3600.13
Avg egl			8.58			0.13%		1701.06

Table 7 Performance of the HGS on low time-dependency instances.

Inst	$ E_R $	BCP LB/Opt	SP T(s)	HGS				T(s)
				Best	Avg	Gap	Gap _{LB}	
C01	79	2417.71	0.93	2423.80	2423.80	0.00%	0.25%	522.30
C02	53	1896.14	0.34	1896.14	1896.14	0.00%	0.00%	140.61
C03	51	1637.80	0.32	1637.80	1637.80	0.00%	0.00%	247.90
C04	72	1996.75	0.69	1996.75	1996.75	0.00%	0.00%	378.12
C05	65	2518.55	0.51	2518.55	2522.22	0.15%	0.15%	210.63
C06	51	1582.08	0.24	1582.08	1582.08	0.00%	0.00%	323.53
C07	52	2118.61	0.42	2118.61	2118.61	0.00%	0.00%	129.54
C08	63	1945.23	0.85	1945.23	1945.23	0.00%	0.00%	182.00
C09	97	3389.81	1.22	3407.54	3408.20	0.02%	0.54%	574.99
C10	55	2207.63	0.59	2207.63	2207.63	0.00%	0.00%	132.52
Avg C			0.61			0.02%	0.09%	284.21
egl-e1	51	1653.19	1.17	1653.19	1653.19	0.00%	0.00%	211.29
egl-e2	72	2388.03	1.47	2392.91	2392.91	0.00%	0.20%	443.84
egl-e3	87	2946.82	1.16	2956.03	2957.30	0.04%	0.36%	811.01
egl-e4	98	3430.98	1.18	3451.16	3451.35	0.01%	0.59%	873.82
egl-s1	75	2378.22	7.07	2381.80	2382.21	0.02%	0.17%	846.49
egl-s2	147	4501.01	6.95	4514.46	4518.89	0.10%	0.40%	1696.38
egl-s3	159	4753.27	7.03	4774.16	4784.27	0.21%	0.65%	2945.21
egl-s4	190	5612.43	7.22	5663.44	5684.34	0.37%	1.28%	3431.32
egl-g1	347	—	26.54	5776.54	5794.02	0.30%	—	3600.16
egl-g2	375	—	27.50	6702.28	6743.45	0.61%	—	3600.17
Avg egl			8.73			0.17%		1845.97

Table 8 Performance of the HGS on medium time-dependency instances.

Inst	$ E_R $	BCP LB/Opt	SP T(s)	HGS				
				Best	Avg	Gap	Gap _{LB}	T(s)
C01	79	2431.77	1.01	2444.24	2444.63	0.02%	0.53%	937.36
C02	53	1889.78	0.35	1889.78	1889.78	0.00%	0.00%	189.71
C03	51	1647.38	0.35	1647.38	1647.38	0.00%	0.00%	398.39
C04	72	2010.97	0.68	2012.42	2012.42	0.00%	0.07%	400.12
C05	65	2505.37	0.53	2505.37	2505.78	0.02%	0.02%	242.49
C06	51	1566.24	0.24	1566.24	1566.24	0.00%	0.00%	331.34
C07	52	2153.38	0.46	2153.38	2153.38	0.00%	0.00%	217.34
C08	63	1959.71	0.88	1959.71	1959.71	0.00%	0.00%	216.92
C09	97	3384.05	1.31	3420.94	3421.60	0.02%	1.11%	927.25
C10	55	2228.00	0.62	2228.00	2228.00	0.00%	0.00%	174.13
Avg C			0.64			0.01%	0.17%	403.50
egl-e1	51	1671.31	1.27	1671.31	1671.31	0.00%	0.00%	289.68
egl-e2	72	2426.65	1.30	2430.55	2430.55	0.00%	0.16%	557.60
egl-e3	87	2969.42	1.27	2978.79	2979.35	0.02%	0.33%	907.83
egl-e4	98	3537.15	1.27	3555.56	3555.65	0.00%	0.52%	1082.23
egl-s1	75	2417.04	7.23	2423.32	2423.32	0.00%	0.26%	754.46
egl-s2	147	4613.70	7.28	4640.30	4653.51	0.28%	0.86%	2171.17
egl-s3	159	4816.24	7.43	4840.15	4855.75	0.32%	0.82%	3461.12
egl-s4	190	5700.98	7.75	5766.76	5784.47	0.31%	1.46%	3600.04
egl-g1	347	—	35.29	5834.33	5849.39	0.26%	—	3600.21
egl-g2	375	—	30.88	6827.08	6846.86	0.29%	—	3600.26
Avg egl			10.10			0.15%		2002.46

Table 9 Performance of the HGS on high time-dependency instances.

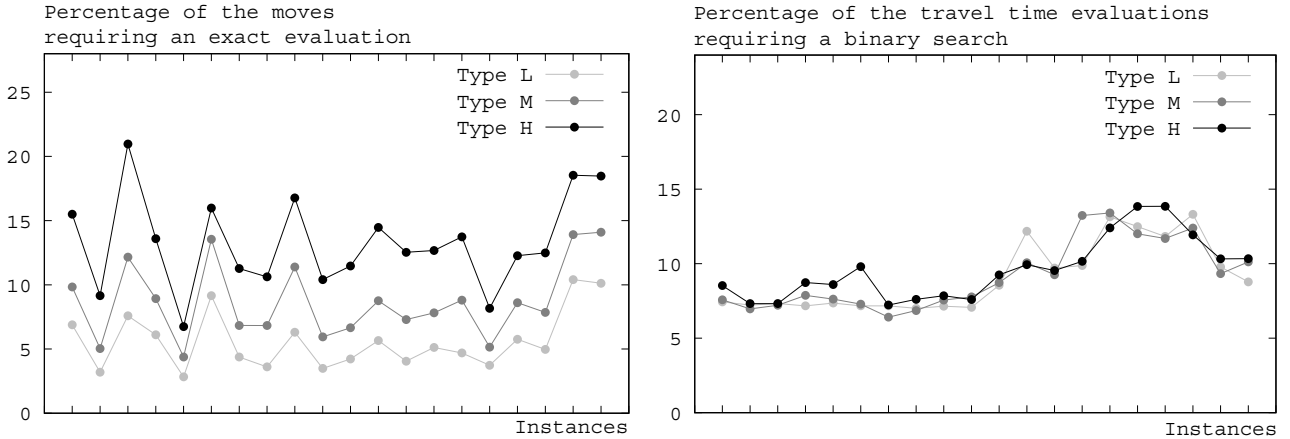


Figure 4 Proportion of filtered moves and avoided binary searches in HGS

As visible in these results, Equation (18) allows to filter 91% of the moves on average. The quality of the lower bounds depends on the amount of time dependency. For low time-dependency instances (type L), 96% of the moves are filtered on average, whereas this number drops to 87% for high time-dependency instances (type H). The bucket structures are also very effective, allowing to complete 90% of the queries without binary search, regardless of the time dependency level.

Both of the previously mentioned components contribute to speed up critical operations representing the bottleneck of the HGS. To highlight more directly their impact, Figure 5 compares the CPU time of HGS on the instances C01–C10 with that of three alternative algorithm variants obtained by deactivating the move filters (HGS-NOF), the bucket data structures (HGS-NOB), or both of those (HGS-NOBF). As shown by this experiment, the use of the move filters diminishes

the computational effort by a factor five, while these two simple techniques jointly reduce the computational time by a factor ten on average, reaching up to 20 for some instances. This time reduction allows to perform a much larger number of iterations within a reasonable time budget, therefore transforming speed-ups into quality gains.

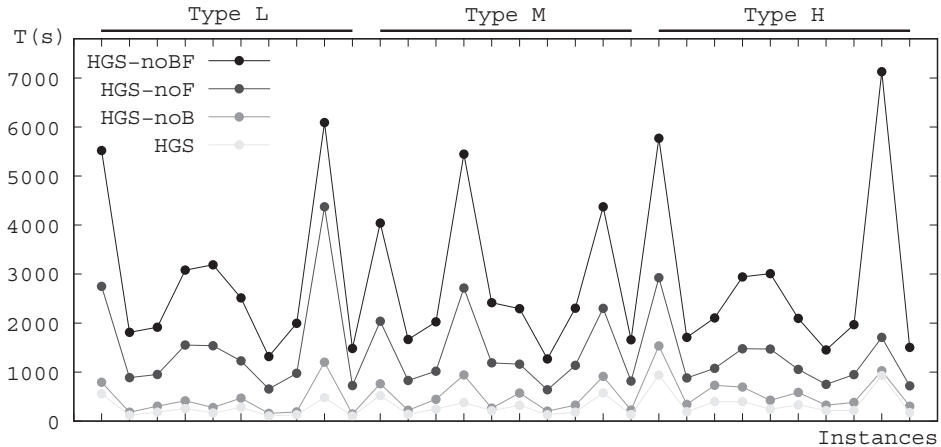


Figure 5 Impact of the move filters and bucket-based function queries on the search time

4.5. The Value of Time-dependent Route and Path Optimization

In a final experiment, we compare the solutions of the TDCARP and CARP algorithms in the presence of inaccurate speed information. For this analysis, we focus on the data sets C01–C10 for each time-dependency level (L, M, and H). For each of these 30 instances, we consider five levels of inaccuracy and generate each time 20 travel-time scenarios by replacing the speed $v_{ij}(t)$ of each travel (and service) speed function piece by a value $v'_{ij}(t) = C v_{ij}(t)$, in which coefficient C is sampled from a truncated normal distribution centered on 1, with standard deviation σ and truncation range $[1 - \sigma, 1 + \sigma]$. Each level of inaccuracy corresponds to a different σ in $\{0.05, 0.1, 0.2, 0.4, 0.6\}$.

We assume that only the original speed information v_{ij} is available to the TDCARP optimization algorithm, whereas the CARP algorithm assumes uniform speed in the network. We measure the average quality of the solutions produced by the two methods over the 20 randomized scenarios. This solution quality is then translated into an average error gap relative to the baseline TDCARP solutions obtained by running HGS with perfect knowledge of the speed conditions v'_{ij} on each scenario. Figure 6 displays the result of this experiment, illustrating the average gap of the two methods on the five groups of scenarios and three instance types. The gap between the CARP and TDCARP solutions is grayed-out on the figure. It represents the value of time-dependent optimization.

As confirmed by these experiments, the accuracy of the speed information has an impact on TDCARP solutions. Inaccurate speed profiles naturally lead to larger gaps relative to the baseline. The grayed-out regions of Figure 6 represent possible improvements that can be achieved by time-dependent routing optimization, whereas the regions below the TDCARP curve represent possible improvements which can arise by improving speed data collection processes.

It is noteworthy that TDCARP solutions always improve upon CARP solutions, even in settings with very inaccurate knowledge of travel speeds (scenario 5 with $\sigma = 0.6$). Indeed, even in those cases, imperfect speed estimates give a better approximation of real scenarios than uniform speeds. Small inaccuracies (e.g., configurations with $\sigma \leq 0.2$) do not reduce the edge of TDCARP optimization,

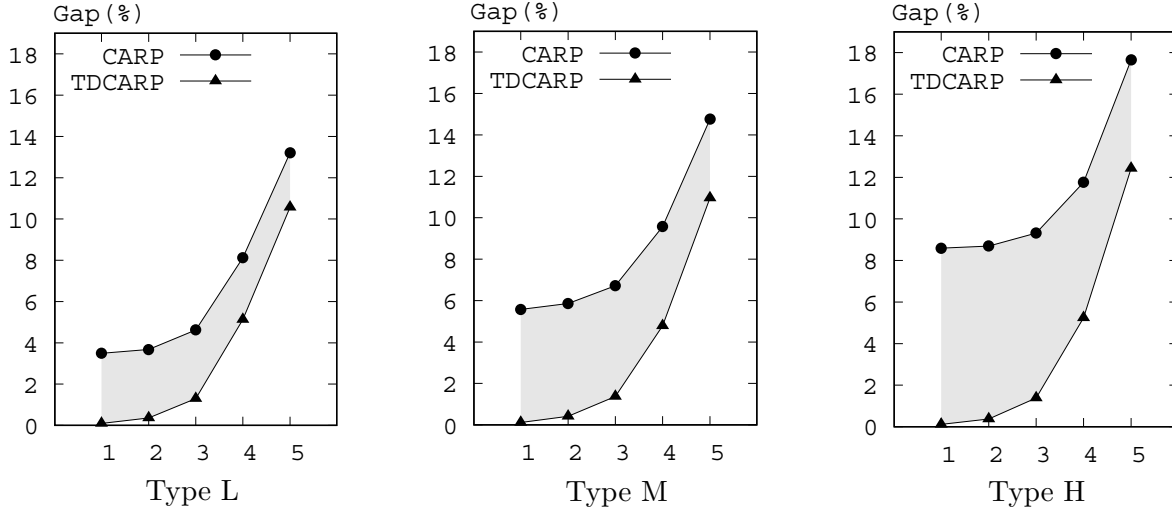


Figure 6 The value of time-dependent routing, considering five level of speed information inaccuracy

with gaps below 1.38% in all cases relatively to the baseline. In contrast, merely omitting time dependency and using average speeds instead leads to a dramatic increase of travel time, which amounts to 6.28% on average for these scenarios, and rises up to 9.32% in high time-dependency cases (type H, scenario 3). Overall, despite data inaccuracies, time-dependent optimization remains essential for a good operational performance.

5. Conclusions and Perspectives

Time-dependent travel times defined at the network level pose significant challenges for solution algorithms. They dramatically increase the (methodological and computational) complexity of travel-time queries and significantly weaken label dominance in column generation-based approaches. Nevertheless, we demonstrated that these challenges can be overcome with dedicated solution strategies, including solution-decoding algorithms, move filters, heuristic dominance, enhanced pricing, and completion bounds. These methodological components allow us to solve small- to medium size-problems to optimality, and to produce good heuristic solutions for larger instances with several hundred services.

Our experiments demonstrate that time-dependent optimization is essential to slash down routing costs, even in scenarios in which speed information is inaccurate. This observation encourages us to use time-dependent routing algorithms in a broader range of applications, including cases with less accurate data sources (Bertsimas et al. 2019).

The research perspectives are numerous. Firstly, our solution evaluations with inaccurate speed assumed that the routes should be fully defined at the start of the operations. As also mentioned in Gendreau et al. (2015), a meaningful research line concerns the investigation of stochastic or dynamic routing problem, in which the travel-speed information collected during the day is used to rearrange customer-visit orders. Secondly, time-dependency dramatically weakens dominance relationships in column generation based methods, now based on simultaneous time and cost comparisons. A similar issue arises when considering generalized vehicle routing problems with time windows in which travel time and cost are not directly proportional (Ben Ticha et al. 2019). New methodological contributions are needed for these problems: better dominance rules, reduced-cost fixing techniques and completion-bounds may help. Finally, although we focused on arc-routing settings, we remind that an adequate management of time-dependent travel times at the network

level remains a key issue for the entire vehicle routing community, and that most of the solution strategies listed in this paper are extensible to this broader context.

Acknowledgments

This research has been partially supported by CAPES, CNPq [grants numbers 308528/2018-2, 313521/2017-4, 425962/2016-4], and FAPERJ [grant number E-26/202.790/2019] in Brazil, as well as the Vietnam National Foundation for Science and Technology Development (NAFOSTED) [grant number 102.99-2016.21]. This support is gratefully acknowledged.

Appendix A: Standard Iterative Algorithm for Arrival-Time Queries

Algorithms 3 and 4 allow to calculate $\Phi_{ij}(t_i)$ and $\Phi_{ij}^{-1}(t_j)$. We denote $v_{ij}(t^-) = \lim_{x \rightarrow t^-} v_{ij}(x)$ and $v_{ij}(t^+) = \lim_{x \rightarrow t^+} v_{ij}(x)$. These algorithms have been commonly used in the time-dependent vehicle routing literature (Ichoua et al. 2003). Their worst case complexity grows linearly with the number of pieces in the speed functions (in $\mathcal{O}(h_{ij})$).

Algorithm 3: Calculation of $\Phi_{ij}(t_i)$

```

 $t \leftarrow t_i$ 
 $d \leftarrow d_{ij}$ 
 $k \leftarrow \arg \min \{x \mid t_x > t_i\}$ 
 $t_j \leftarrow t + d/v_{ij}(t^+)$ 
while  $t_j > t_k$  do
   $d \leftarrow d - v_{ij}(t^+) \times (t_k - t)$ 
   $t \leftarrow t_k$ 
   $k \leftarrow k + 1$ 
   $t_j \leftarrow t + d/v_{ij}(t^+)$ 
return  $t_j$ 

```

Algorithm 4: Calculation of $\Phi_{ij}^{-1}(t_j)$

```

 $t \leftarrow t_j$ 
 $d \leftarrow d_{ij}$ 
 $k \leftarrow \arg \max \{x \mid t_x < t_j\}$ 
 $t_i \leftarrow t - d/v_{ij}(t^-)$ 
while  $t_i < t_k$  do
   $d \leftarrow d - v_{ij}(t^-) \times (t - t_k)$ 
   $t \leftarrow t_k$ 
   $k \leftarrow k - 1$ 
   $t_i \leftarrow t - d/v_{ij}(t^-)$ 
return  $t_i$ 

```

Appendix B: Title Appendix B

In the following examples, we demonstrate that time differences can arbitrarily diminish over a path. Consider two partial paths P_1 and P_2 currently finishing on the same service arc (1, 2) with $\Phi(P_1) = 1$ and $\Phi(P_2) = 5$. Both paths are extended on a sequence of three additional services (2, 3) \rightarrow (3, 4) \rightarrow (4, 5) with service-and-travel speed functions defined as:

$$\hat{v}_{23}(t) = \begin{cases} 1 & \text{if } t \in [0, 5] \\ 2 & \text{otherwise} \end{cases} \quad \hat{v}_{34}(t) = \begin{cases} 1 & \text{if } t \in [0, 7] \\ 2 & \text{otherwise} \end{cases} \quad \hat{v}_{45}(t) = \begin{cases} 1 & \text{if } t \in [0, 8] \\ 2 & \text{otherwise} \end{cases}$$

With these parameters, label P_1 will complete the services to (2, 3), (3, 4) and (4, 5) at time 5, 7 and 8 respectively, whereas label P_2 will complete the same services at time 7, 8 and 8.5. The original time difference of $\Delta = 4$ units between the two labels has been reduced to 0.5 units only after three services, and a trivial generalization of this example shows that it can diminish to $\Delta \left(\frac{v_{\min}}{v_{\max}}\right)^x$ after x service or travel links, where v_{\min} and v_{\max} are the minimum and maximum possible speed values (here $v_{\min} = 1$ and $v_{\max} = 2$).

References

- Baldacci, R., A. Mingozzi, R. Roberti. 2011. New route relaxation and pricing strategies for the vehicle routing problem. *Operations Research* **59**(5) 1269–1283.
- Bartolini, E., J.-F. Cordeau, G. Laporte. 2013. Improved lower bounds and exact algorithm for the capacitated arc routing problem. *Mathematical Programming* **137**(1) 409–452.

-
- Bast, H., D. Delling, A. Goldberg, M. Müller-Hannemann, T. Pajor, P. Sanders, D. Wagner, R.F. Werneck. 2016. Route planning in transportation networks. L. Kliemann, P. Sanders, eds., *Algorithm Engineering: Selected Results and Surveys*. Springer, Berlin Heidelberg, 19–80.
- Batz, G.V., R. Geisberger, P. Sanders, C. Vetter. 2013. Minimum time-dependent travel times with contraction hierarchies. *Journal of Experimental Algorithmics* **18**(1) 1–43.
- Belenguer, J.M., E. Benavent. 1998. The capacitated arc routing problem: Valid inequalities and facets. *Computational Optimization and Applications* **10**(2) 165–187.
- Ben Ticha, H., N. Absi, D. Feillet, A. Quilliot. 2019. Multigraph modeling and adaptive large neighborhood search for the vehicle routing problem with time windows. *Computers & Operations Research* **104**(1) 113–126.
- Bertsimas, D., A. Delarue, P. Jaillet, S. Martin. 2019. Travel time estimation in the age of big data. *Operations Research* **67**(2) 498–515.
- Buellens, P., L. Muyldermans, D. Cattrysse, D. Van Oudheusden. 2003. A guided local search heuristic for the capacitated arc routing problem. *European Journal of Operational Research* **147**(3) 629–643.
- Black, D., R. Eglese, S. Wöhlk. 2013. The time-dependent prize-collecting arc routing problem. *Computers & Operations Research* **40**(2) 526–535.
- Brandão, J., R. Eglese. 2008. A deterministic tabu search algorithm for the capacitated arc routing problem. *Computers & Operations Research* **35**(4) 1112–1126.
- Cattaruzza, D., N. Absi, D. Feillet, J. González-Feliu. 2017. Vehicle routing problems for city logistics. *EURO Journal on Transportation and Logistics* **6**(1) 51–79.
- Cookson, G., B. Pishue. 2018. INRIX Global Traffic Scorecard. Tech. rep., INRIX Research.
- Corberán, Á, G Laporte. 2015. *Arc routing: Problems, methods, and applications*. Society for Industrial and Applied Mathematics, Philadelphia, PA, USA.
- Eglese, R., W. Maden, A. Slater. 2006. A road timetable to aid vehicle routing and scheduling. *Computers & Operations Research* **33**(12) 3508–3519.
- Foschini, L., J. Hershberger, S. Suri. 2014. On the complexity of time-dependent shortest paths. *Algorithmica* **68**(4) 1075–1097.
- Gendreau, M., G. Ghiani, E. Guerriero. 2015. Time-dependent routing problems: A review. *Computers & Operations Research* **64** 189–197.
- Ghiani, G., E. Guerriero. 2014. A note on the Ichoua, Gendreau, and Potvin (2003) travel time model. *Transportation Science* **48**(3) 458–462.
- Hershberger, J. 1989. Finding the upper envelope of n line segments in $O(n \log n)$ time. *Information Processing Letters* **33**(4) 169–174.
- Herszterg, I., M. Poggi, T. Vidal. 2019. Two-dimensional phase unwrapping via balanced spanning forests. *INFORMS Journal on Computing* **31**(3) 527–543.
- Huang, Y., L. Zhao, T. Van Woensel, J.-P. Gross. 2017. Time-dependent vehicle routing problem with path flexibility. *Transportation Research Part B: Methodological* **95** 169–195.
- Ichoua, S., M. Gendreau, J.-Y. Potvin. 2003. Vehicle dispatching with time-dependent travel times. *European Journal of Operational Research* **144**(2) 379–396.
- Irnich, S. 2008. Solution of real-world postman problems. *European Journal of Operational Research* **190**(1) 52–67.
- Jaballah, R., M. Veenstra, L.C. Coelho, J. Renaud. 2019. The time-dependent shortest path and vehicle routing problem. Tech. rep., CIRRELT-2019-12.
- Laporte, G., S. Ropke, T. Vidal. 2014. Heuristics for the vehicle routing problem. P. Toth, D. Vigo, eds., *Vehicle Routing: Problems, Methods, and Applications*, chap. 4. Society for Industrial and Applied Mathematics, 87–116.
- Lera-Romero, G., J.J. Miranda Bront, F.J. Soulignac. 2020. Linear edge costs and labeling algorithms: The case of the time-dependent vehicle routing problem with time windows. *Networks, Forthcoming* .

- Li, L.Y.O., R.W. Eglese. 1996. An interactive algorithm for vehicle routing for winter-gritting. *Journal of the Operational Research Society* **47**(2) 217–228.
- Maden, W., R. Eglese, D. Black. 2009. Vehicle routing and scheduling with time-varying data: A case study. *Journal of the Operational Research Society* **61**(3) 515–522.
- Martinelli, R., D. Pecin, M. Poggi. 2014. Efficient elementary and restricted non-elementary route pricing. *European Journal of Operational Research* **239**(1) 102 – 111.
- Mecler, J., A. Subramanian, T. Vidal. 2019. A simple and effective hybrid genetic search for the job sequencing and tool switching problem. Tech. rep., PUC-Rio, ArXiv:1910.10021.
- Orda, A., R. Rom. 1990. Shortest-path and minimum-delay algorithms in networks with time-dependent edge-length. *Journal of the Association for Computing Machinery* **37**(3) 607–625.
- Pecin, D., E. Uchoa. 2019. Comparative analysis of capacitated arc routing formulations for designing a new branch-cut-and-price algorithm. *Transportation Science* **53**(6) 1673–1694.
- Pessoa, A., E. Uchoa, M. Poggi, R. Rodrigues. 2010. Exact algorithm over an arc-time-indexed formulation for parallel machine scheduling problems. *Mathematical Programming Computation* **2**(3) 259–290.
- Rincon-Garcia, N., B.J. Waterson, T.J. Cherrett. 2018. Requirements from vehicle routing software: Perspectives from literature, developers and the freight industry. *Transport Reviews* **38**(1) 117–138.
- Røpke, S. 2012. Branching decisions in branch-and-cut-and-price algorithms for vehicle routing problems. Presentation, International Workshop on Column Generation, June 13, Bromont, QC, Canada.
- Sun, J., Y. Meng, G. Tan. 2015. An integer programming approach for the Chinese postman problem with time-dependent travel time. *Journal of Combinatorial Optimization* **29**(3) 565–588.
- Toffolo, T.A.M., T. Vidal, T. Wauters. 2019. Heuristics for vehicle routing problems: Sequence or set optimization? *Computers & Operations Research* **105** 118–131.
- Vidal, T. 2017. Node, edge, arc routing and turn penalties: Multiple problems – One neighborhood extension. *Operations Research* **65**(4) 992–1010.
- Vidal, T., M. Battarra, A. Subramanian, G. Erdogan. 2015a. Hybrid metaheuristics for the clustered vehicle routing problem. *Computers & Operations Research* **58**(1) 87–99.
- Vidal, T., T.G. Crainic, M. Gendreau, C. Prins. 2013. Heuristics for multi-attribute vehicle routing problems: A survey and synthesis. *European Journal of Operational Research* **231**(1) 1–21.
- Vidal, T., T.G. Crainic, M. Gendreau, C. Prins. 2014. A unified solution framework for multi-attribute vehicle routing problems. *European Journal of Operational Research* **234**(3) 658–673.
- Vidal, T., T.G. Crainic, M. Gendreau, C. Prins. 2015b. Timing problems and algorithms: Time decisions for sequences of activities. *Networks* **65**(2) 102–128.
- Vidal, T., G. Laporte, P. Matl. 2020. A concise guide to existing and emerging vehicle routing problem variants. *European Journal of Operational Research*, *Forthcoming* .
- Vidal, T., N. Maculan, L.S. Ochi, P.H.V. Penna. 2016. Large neighborhoods with implicit customer selection for vehicle routing problems with profits. *Transportation Science* **50**(2) 720–734.
- Yu, V.F., S.-W. Lin. 2015. Iterated greedy heuristic for the time-dependent prize-collecting arc routing problem. *Computers and Industrial Engineering* **90** 54–66.